C. S. Fraser*
S. A. Veress
Department of Civil Engineering
University of Washington
Seattle, WA 98195

Self-Calibration of a Fixed-Frame Multiple-Camera System

A simultaneous multiple-camera self-calibrating bundle adjustment has been employed.

Abstract: *The self-calibration of a fixed-frame multiple-camera system used for close-range photogrammetric research in the fields of biomedicine and bioengineering at the University of Washington is detailed. In order to carry out this system calibration, a simultaneous multiple-camera self-calibrating bundle adjustment has been employed. The incorporation of mixed block- and camera-invariant additional parameter sets in the functional model of self-calibration is outlined. An experimental calibration of the fixed-frame photogrammetric system involving a three-camera, ten-photo self-calibration adjustment is described and results of this experiment are discussed. Findings from this investigation indicate that the simultaneous multiple-camera self-calibration technique outlined is a useful and practical method for dual- and multiple-camera photogrammetric system calibration.*

Recent developments in the field of precise close-range photogrammetry have included the use of dual- and multiple-camera systems. The adoption of such systems has been especially apparent in photogrammetric surveys where the subject, or object, being imaged is in a dynamic mode. Dynamic photogrammetric surveys employing multiple-camera systems have been widely applied in the disciplines of biomedicine and bioengineering. At the University of Washington a fixed-frame multiple-camera system has been developed for such applications. Veress and Tiwari (1976) have reported wide usage of this system by the departments of Orthopaedics, Orthodontics, Dentistry, and Civil Engineering. Recently, the fixed-frame was moved from its original location to the photogrammetric laboratory in the Department of Civil Engineering and it was thus necessary to carry out a system recalibration. The recovery of the inner cone parameters of the three MK-70 Hasselblad cameras comprising the camera system and the recovery of calibration data for the reference frame, through a simultaneous multiple-camera self-calibration, form the subject of this paper.

Over the past decade the feasibility and advantages—both theoretical and practical—of the self-calibrating bundle adjustment technique of photogrammetric system calibration have been clearly established. As a result, the method has achieved wide acceptance in both the areas of close-range photogrammetry and traditional aerial triangulation. For the calibration of the close-range fixed-frame multiple-camera system, it was decided to employ such a method. However, the use of multiple cameras gives rise to the need for an algorithmic extension to the traditional single-camera form of the self-calibrating bundle adjustment. In the following sections the development of a practical simultaneous multiple-camera self-calibration method is detailed, the application of the method to the fixed-frame system calibration is described, and the results obtained are discussed.

Theoretical Background

Self-Calibration Model

The general normal equations for the self-calibrating bundle adjustment are given in the form of the parametric system

* Now at the Department of Civil Engineering, University of Canterbury, Christchurch 1, New Zealand.

Photogrammetric Engineering and Remote Sensing,
Vol. 46, No. 11, November 1980, pp. 1439-1445.

$$\begin{bmatrix} \dot{B}^T\dot{W}\dot{B} + \dot{W} & \dot{B}^T\dot{W}\ddot{B} & \dot{B}^T\dot{W}\dddot{B} \\ & \ddot{B}^T\dot{W}\ddot{B} + \ddot{W} & \ddot{B}^T\ddot{W}\dddot{B} \\ \text{symmetric} & & \dddot{B}^T\dddot{W}\dddot{B} + \dddot{W} \end{bmatrix} \begin{bmatrix} \dot{\delta} \\ \ddot{\delta} \\ \dddot{\delta} \end{bmatrix} = \begin{bmatrix} \dot{B}^T\dot{W}e - \dot{W}\dot{e} \\ \ddot{B}^T\ddot{W}e - \ddot{W}\ddot{e} \\ \dddot{B}^T\dddot{W}e - \dddot{W}\dddot{e} \end{bmatrix} \tag{1}$$

where

$\dot{\delta}, \ddot{\delta}, \dddot{\delta}$ represent the vectors of corrections to the exterior orientation elements, the object space coordinates, and the additional parameters which comprise the systematic image error correction model;

$\dot{B}, \ddot{B}, \dddot{B}$ refer to the matrices of partial derivatives of the extended collinearity equations with respect to the exterior orientation elements, the object space coordinates, and the additional parameters;

$e, \dot{e}, \ddot{e}, \dddot{e}$ indicate the discrepancy vectors; and

$W, \dot{W}, \ddot{W}, \dddot{W}$ are the weight matrices.

In the normal equation system, Equation 1, all parameters are treated as observed or pseudo-observed quantities subject to a priori constraints, as indicated by the block-diagonal weight matrices $\dot{W}$, $\ddot{W}$, and $\dddot{W}$.

ADDITIONAL PARAMETERS

The additional parameter vector, $\dddot{\delta}$, is comprised of the parameters of the inner cone of the camera, or cameras, and parameters which form the correction model for the systematic image coordinate errors due to other physical, mechanical, and chemical factors. Parameters in the latter group are essentially empirical in nature, whereas parameters in the former group represent an analytical model for lens distortion, both radial and decentering, and perturbations in the elements of interior orientation. For the present application, the following additional parameter model has been adopted for the image coordinate corrections, Δx and Δy:

$$\begin{aligned} \Delta x &= \Delta x_c + \Delta x_b \\ \Delta y &= \Delta y_c + \Delta y_b \end{aligned} \tag{2}$$

Here, Δx_c and Δy_c contain correction terms which relate to a specific inner cone parameter set, whereas Δx_b and Δy_b represent the empirical image deformation correction model. In expanded form, Δx_c and Δy_c are given for a single camera i by the equations

$$\begin{aligned} \Delta x_c &= x(K_{i1}r^2 + K_{i2}r^4 + K_{i3}r^6) \\ &\quad + P_{i1}(3x^2 + y^2) + 2P_{i2}xy + (-x/c_i)dc_i - x_{oi} \end{aligned} \tag{3}$$

$$\begin{aligned} \Delta y_c &= y(K_{i1}r^2 + K_{i2}r^4 + K_{i3}r^6) + 2P_{i1}xy \\ &\quad + P_{i2}(x^2 + 3y^2) + (-y/c_i)dc_i - y_{oi} \end{aligned}$$

where

$$\begin{aligned} x &= x' - x_{oi} \\ y &= y' - y_{oi} \\ r &= (x^2 + y^2)^{1/2} \end{aligned}$$

and

x', y' are the observed image coordinates;

x_{oi}, y_{oi} are the coordinates of the principal point of camera i;

c_i is the Gaussian focal length of camera i;

dc_i is the correction to c_i;

K_{i1}, K_{i2}, K_{i3} are the coefficients of symmetric radial distortion; and

P_{i1}, P_{i2} are the decentering distortion coefficients.

For a multiple camera self-calibration, the inner cone parameters $K_{i1}, K_{i2}, K_{i3}, P_{i1}, P_{i2}, dc_i, x_{oi}$, and y_{oi} will be camera-invariant.

The corrections Δx_b and Δy_b can be represented by a number of terms of the following general polynomials:

$$\begin{Bmatrix} \Delta x_b \\ \Delta y_b \end{Bmatrix} = \sum_{i=0}^{n} \sum_{j=0}^{n-i} \begin{Bmatrix} a_{ij} \\ b_{ij} \end{Bmatrix} x^i y^j \tag{4}$$

The expressions for Δx_b and Δy_b adopted for the present investigation are given in expanded form by

$$\begin{aligned} \Delta x_b &= +a_1xy + a_2y^2 + a_3x^2y + a_4xy^2 \\ \Delta y_b &= +b_1x + b_2y + b_3xy + b_4x^2 + b_5x^2y + b_6xy^2 \end{aligned} \tag{5}$$

In Equation 5, the linear terms in x and y account for a lack of orthogonality and a differential scale component between the image coordinate axes. Schut (1978) has reported that it is immaterial whether the two linear terms are used to correct x, y, or both. The large depth of spacing typically encountered in close-range object target arrays makes it appropriate to retain the terms a_1xy and b_3xy rather than the two omitted second-order terms in x^2 and y^2. Gotthardt (1975) has presented an illustration of the geometric effect of each of the empirical terms in Equation 5 for an image having a standard 3 by 3 point configuration. The combined analytical and empirical additional parameter model approach to self-calibration has been adopted by a number of investigators (see, for example, Brown, 1974; Brown, 1976; Salmenperä *et al.*, 1974). For the present application, which emphasizes the recovery of inner cone parameters of a multiple-camera system, alternative formulations of the image correction model incorporating orthogonal polynomials (Ebner, 1976;

Grün, 1978) or harmonic functions (El Hakim and Faig, 1979) have not been considered.

Whereas the inner cone parameters are camera-invariant in a simultaneous multiple-camera self-calibration, the empirical image deformation parameters can be camera-invariant, block-invariant in nature, or related to a single photographic image. In a case where all images are recorded on the same role of film, it is not unreasonable to assume that there will be a component of film deformation—say longitudinal stretching or lateral shrinkage—common to all photographs. A further, albeit less typical, example of the need to include block-invariant additional parameters is where comparator errors are suspected and all image coordinates are observed on the same comparator. In the present investigation, all photographs were recorded on the same role of film and image coordinate observations were carried out on the one comparator. For this reason it was decided to treat the empirical additional parameters as being block-invariant. The computational algorithm was constructed, however, so as to accommodate mixed block-, camera-, and image subset-invariant parameter sets.

STRUCTURE OF THE MATRIX OF ADDITIONAL PARAMETERS

The coefficient matrix, $\ddot{\boldsymbol{B}}_j^{(i)}$ for a single image point observation, j, on an image recorded with camera, i, will have dimensions of 2 by 18 if all parameters of the image correction model, Equation 2, are included. Further, this matrix can be represented in the form of two submatrices: the coefficient matrix of the parameters of the inner cone of camera i, $\ddot{\boldsymbol{B}}_{cj}^{(i)}$, and the coefficient matrix of the block-invariant parameters, $\ddot{\boldsymbol{B}}_{bj}^{(i)}$. In a simultaneous multiple-camera self-calibration there must be no linear dependence between the parameters of the different submatrices $\ddot{\boldsymbol{B}}_{cj}^{(i)}$ for the individual cameras. On the other hand, the block-invariant parameters, with coefficient matrix $\ddot{\boldsymbol{B}}_{bj}^{(i)}$, will be common to all photographic images.

The structure of the resulting additional parameter matrix, $\ddot{\boldsymbol{B}}_j$, for a single point, j, can be illustrated by considering the case where the image point is seen on three photographs, each from a different camera. The matrix $\ddot{\boldsymbol{B}}_j$ will then assume the form

$$\ddot{\boldsymbol{B}}_j = \left[\begin{array}{ccc|c} \ddot{\boldsymbol{B}}_{cj}^{(1)} & 0 & 0 & \ddot{\boldsymbol{B}}_{bj}^{(1)} \\ 0 & \ddot{\boldsymbol{B}}_{cj}^{(2)} & 0 & \ddot{\boldsymbol{B}}_{bj}^{(2)} \\ 0 & 0 & \ddot{\boldsymbol{B}}_{cj}^{(3)} & \ddot{\boldsymbol{B}}_{bj}^{(3)} \end{array}\right] \qquad (6)$$

If a total of k_c camera-invariant and k_b block-invariant additional parameters are used in the formation of $\ddot{\boldsymbol{B}}_j$, the resulting normal equation submatrix $\ddot{\boldsymbol{B}}^T\boldsymbol{W}\ddot{\boldsymbol{B}}_j$ (see Equation 1) will be block-diagonal with dimensions k_c by k_c, symmetrically bordered by a border of width k_b.

The Fixed-Frame Multiple-Camera System

REFERENCE FRAME

Veress and Tiwari (1976) have given a complete description of the design and fabrication of the fixed-frame, as well as an introduction to the methodology adopted for the multiple-camera system. Here, important aspects of the design criteria of the frame and the geometrical arrangements of the camera stations are summarized.

The reference frame has been designed to accommodate both fixed-base stereo and convergent photography. It is manufactured from steel tubes pressed into solid joints, with the final structure being triangular shaped with a base length of 2 m and a height of 2.1 m. Fixed camera stations have been located on the frame according to a design criterion whereby the system has a sufficiently favorable geometry to allow for specimen sizes from 2 cm upwards in the object field. Figure 1 illustrates the camera station locations on the frame.

The camera locations numbered 1, 2, and 3 in Figure 1 form the convergent stations, the angle between the normal to the frame and the camera axes being 22° at stations 1 and 2, and 38° at station

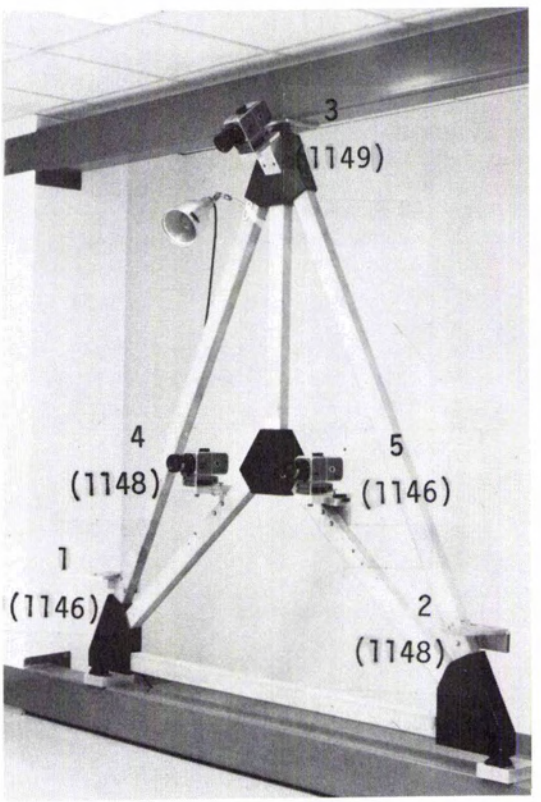

FIG. 1. Camera locations on the fixed-frame.

3. Camera stations 4 and 5 are established with a base of 611 mm in such a way that the camera axes are parallel and collinear to the normal to the plane of the frame.

CAMERA SYSTEM

The camera system consists of three MK-70 metric Hasselblad cameras, each with a Biogon *f*/5.6 60 mm lens. Each camera is distinguished by its serial number: 1146, 1148, and 1149. The former two of these are a factory matched pair especially produced for this system. The MK-70 incorporates a calibrated reseau plate with 25 crosses in a 1 by 1 cm grid pattern. All three cameras have been factory calibrated at infinity focus. Figure 2 shows the camera 1148 mounted on platform number 4 of the reference frame.

Precisely machined plates have been affixed to the base of each camera so that on successive removal and replacement of a camera on its respective platform, the same position is recaptured to within a tolerance of a few tens of micrometres (see Figure 2). The camera numbers listed at each location in Figure 1 indicate the configuration adopted for the present experiment. The derived exposure station coordinates are therefore only applicable in situations where the same camera configuration is used.

Self-Calibration Application

AUXILIARY CAMERA STATIONS

For the successful recovery of the inner cone parameters of the MK-70 cameras comprising the multiple-camera system, a favorable geometric configuration for the camera stations and the object target field is required. Among the well-established factors that must be considered is that the coordinates of the principal point can typically only be determined if there is at least one pair of well spread swing angles between the exposure stations for each camera. Further, the Gaussian focal length can usually be treated as an unknown only in cases where the photography is highly convergent and/or there is a significant depth of spacing within the object target field.

For the above mentioned reasons alone it was necessary to incorporate auxiliary camera stations at five locations away from the reference frame, one each for cameras 1149 and 1148 and three for camera 1146. The positioning of the additional exposure stations enhanced the geometric strength of the camera configuration and allowed for the introduction of nominally orthogonal swing angles. A plan view showing the location of each auxiliary exposure station and the serial number of the camera occupying that station is presented in Figure 3. Also shown in the figure are the adopted kappa rotation angles and approximate fields of view at each auxiliary location.

TARGET FIELD

The object space target field established for the self-calibration consisted of four piano wires suspended as plumb lines, each weighted with a heavy plumb bob immersed in an oil bath. Small spherical seed-beads of approximately 3 mm diameter were fixed on the wires to serve as target points. In all, 34 targets were established; however, images of all the object points did not appear on all the ten photographs.

The configuration of the target field is illustrated in Figure 3. The outer wires are 1.78 m apart and located at 2.2 m from the reference frame. The inner pair of wires have a separation of 0.62 m and are situated at 1.65 m from the frame. In order to constrain the origin, scale, and orientation of this system, seven coordinate values were held fixed in the subsequent adjustments (standard error = ± 1 μm). Scale was determined by precisely measuring the separation of the two inner wires,

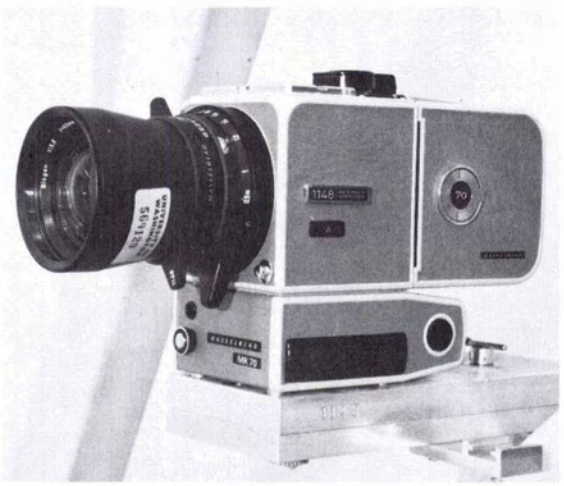

FIG. 2. The Hasselblad MK-70 and mount.

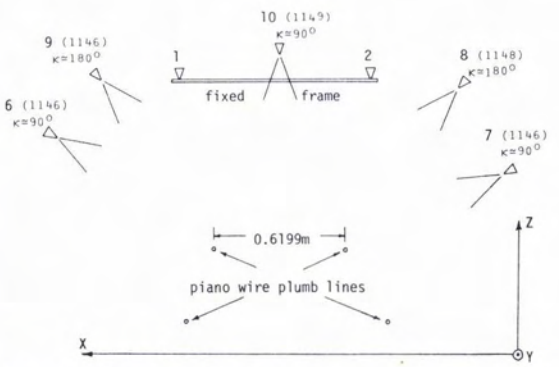

FIG. 3. Plan view illustrating the configuration of the auxiliary camera stations and the object target array.

the measured distance being 0.6199 m. The coordinate axes were defined as X in the direction of the line joining the two inner wires, Y collinear with the local vertical, and Z mutually at right angles to X and Y, positive toward the frame, as shown in Figure 3.

PHOTOGRAPHIC PROCEDURE

Adopted camera settings for the photography were as follows: an exposure time of 1/2 sec. at f-stop 22, with all cameras focused at 2 m. At f-stop 22 the depth of field was large enough so that all image points were in acceptably clear focus. The ten photographs were exposed on the same role of film over a 30 minute period.

DATA COLLECTION AND REDUCTION

Image coordinate observations were carried out on an OMI-Bendix AP/C analytical plotter at the University of Washington, with each negative being viewed monocularly. In addition to measuring the x, y coordinates of all target points which were clearly definable, the coordinates of eight reseau crosses were observed.

Preliminary data preparation and reduction for the self-calibrating bundle adjustment program SELCAL used for the multiple-camera self-calibration was carried out by a preprocessing program called PREPRO. The five major roles of PREPRO are as follows:

- Reads the observed and preliminary estimate data;
- Carries out the two-dimensional coordinate transformation, the preliminary corrections for lens distortion (radial and decentering), and the corrections for interior orientation perturbations;
- Computes a general space resection for each photo from given points in order to obtain refined initial approximations for the elements of exterior orientation;
- Computes space intersections for required object points in order to obtain initial approximations for input to the final self-calibration adjustment; and
- Sets up a point-wise ordered data file which forms the input to SELCAL.

SELF-CALIBRATION ADJUSTMENTS

In order to obtain the optimum recovery of calibration parameters for the three MK-70 Hasselblads, a number of multiple-camera self-calibrating bundle adjustments were carried out. Various combinations of camera- and block-invariant parameters were used in the adjustments and an indication of the most favorable additional parameter model was gained by considering both the root mean square (RMS) values of the image coordinate residuals and the statistical significance of the individual additional parameters. In the ten self-calibration adjustments carried out, the RMS values, $s_{x,y}$ ranged from ± 3.3 μm to ± 4.0 μm, with the optimum solution yielding RMS estimates of $s_x = \pm 3.2$ μm and $s_y = \pm 3.4$ μm.

The following image correction model was found to produce the most favorable self-calibration solution from the points of view of statistical significance and the minimization of the RMS values of image coordinate residuals:

$$\begin{aligned} \Delta x_c &= xr^2K_{i1} + xr^4K_{i2} + (-x/c_i)dc_i + (3x^2 + y^2)P_{i1} \\ &\quad + 2xyP_{i2} - x_{oi} \\ \Delta y_c &= yr^2K_{i1} + yr^4K_{i2} + (-y/c_i)dc_i + 2xyP_{i1} \\ &\quad + (x^2 + 3y^2)P_{i2} - y_{oi} \end{aligned} \tag{7}$$

and

$$\begin{aligned} \Delta x_b &= a_4xy^2 \\ \Delta y_b &= b_2y + b_6xy^2 \end{aligned} \tag{8}$$

The inclusion of the seventh-order radial distortion polynomial coefficient in the camera-invariant additional parameter set was found to yield an excessively high correlation between the parameters K_{i2} and K_{i3}, indicating a strong linear dependence or duplication of roles. In addition, the combination of the coefficients K_{i1} and K_{i3} produced poorer a posteriori precision for the lens distortion function than the combination of K_{i1} and K_{i2}. These findings were consistent with a previously conducted investigation (Fraser, 1980) and it was decided to eliminate the parameter K_{i3} from the camera-invariant additional parameter set for each camera.

Statistical tests indicated that the first-order scale parameter b_2 and the two third-order parameters a_4 and b_6 were the only significantly nonzero parameters of the block-invariant image correction model at a significance level of 5 percent. This suggests that to a large degree the linearized projective equations used for the initial image coordinate transformations accounted for the second-order film deformation.

RESULTS OF SYSTEM SELF-CALIBRATION

CAMERA CALIBRATION PARAMETERS

In the following paragraphs the results of the optimum self-calibration adjustment conducted are outlined. The parameters of the inner cone of each camera were recovered, although these parameters were not all statistically significant at the specified confidence level.

Radial Lens Distortion. The symmetric radial lens distortion curves obtained in the multiple-camera self-calibration are illustrated in Figure 4. For the examination of the significance of the distortion polynomials, a multivariate linear hypothesis testing procedure was adopted because of the strong correlation existing between the coefficients, K_{i1} and K_{i2}. The individual tests for cameras 1149 and 1148 indicated that neither distortion polynomial was significant at the 5 percent level. The lack of a significant distortion curve at a focal

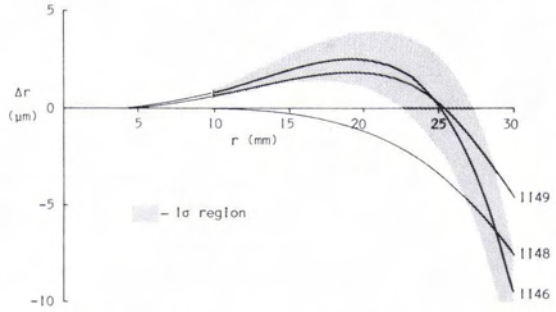

FIG. 4. Radial lens distortion curves.

setting of 2 m may imply one of three things: first, that the lens is distortion free from a practical point of view; second, that no significant trend could be identified because of the inherently large pseudo-random errors due to anomalous film deformation; and third, that there were insufficient degrees of freedom in the multiple-camera adjustment. A combination of the latter two points provides the most probable explanation, for only two exposures were taken with camera 1149 and three with camera 1148.

For camera 1146, the null hypothesis of rank 2 that the radial lens distortion coefficients were equal to zero had to be rejected at the 5 percent level and, thus, the derived polynomial was deemed to be significant. The 1σ region about the distortion curve for camera 1146 is shown in Figure 4, where the a posteriori standard error reaches a magnitude of 2.8 μm at a radius of 30 mm.

Decentering Distortion. Figure 5 illustrates the decentering profiles determined for each of the three cameras. The phase angle, ϕ_0, of the axis of maximum tangential distortion for each camera and the 1σ limit on the tangential profile for camera 1146 are also shown in the figure. Of the three profiles, only that of camera 1149 is statistically significant at a 5 percent level. However, even though they are not significant, the tangential profiles and phase angles determined for the cameras 1146 and 1148 are remarkably similar, even considering the fact that they are a factory matched pair. An earlier, statistically significant determination of P_{i1} and P_{i2} for camera 1146 at a focal setting of 2 m (Fraser, 1980) produced both a profile and phase angle consistent with those illustrated in Figure 5.

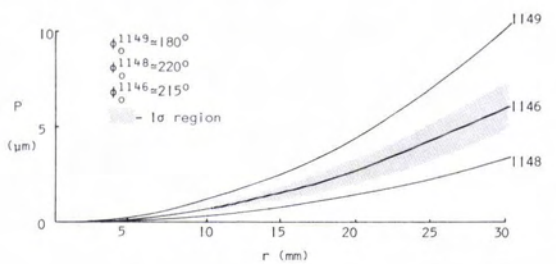

One feature recognized in this multiple-camera self-calibration, which has previously been recognized by Brown (1972), was the high correlation between the decentering distortion coefficients, P_{i1} and P_{i2}, and the interior orientation elements, x_{oi} and y_{oi}. The degree of this coupling appears to be inversely proportional to object target point density.

Interior Orientation Parameters. The adjusted values for the coordinates of the principal point, determined at a focal setting of 2 m, gave rise to some initial concern; in all cases they were substantially different from the factory calibrated values at infinity focus. The discrepancies range from −0.019 to 0.203 mm, yet the largest a posteriori standard error of a self-calibrated value is $\sigma_{x_{oi}} \simeq \sigma_{y_{oi}} \simeq \pm 0.030$ mm for camera 1149. One explanation for the discrepancy between the factory calibrated and the self-calibrated values is that the lens barrels of the cameras are misaligned such that the optical axis is not normal to the film plane. However, a subsequent self-calibration for camera 1146 indicated that such a misalignment was not present. The discrepancies must therefore be put down to errors in the factory calibration or to movement of the reseau plate subsequent to the initial calibration.

Because the three cameras had only been factory calibrated at infinity focus, a priori estimates for the principal distances at a focal setting of 2 m were obtained by using the thin lens equation. The adjusted Gaussian focal lengths differed somewhat from the initial estimates, with the respective values for the factory matched pair being $c_{1146} = 63.32$ mm and $c_{1148} = 63.27$ mm. The a posteriori standard error of each of the three adjusted principal distances was about ±0.020 mm.

THE REFERENCE FRAME

From an examination of the a posteriori variance-covariance matrix obtained from the 10 photo, three-camera self-calibration adjustment, it was apparent that the a posteriori standard errors of both the exterior orientation angles, ω, ϕ, and κ, and the object space exposure station coordinates, X^c, Y^c, and Z^c, for each camera platform were of similar magnitude. The derived estimates of precision closely approximated the following values:

$$\sigma_{Xc} \simeq \pm 0.035 \text{ cm}, \quad \sigma_{\omega} \simeq \pm 90''$$
$$\sigma_{Yc} \simeq \pm 0.040 \text{ cm}, \quad \sigma_{\phi} \simeq \pm 90''$$
$$\sigma_{Zc} \simeq \pm 0.050 \text{ cm}, \quad \sigma_{\kappa} \simeq \pm 30''$$

The precision of the adjusted object target points was dependent on their position with respect to the three targets whose fixed coordinates ($2 \times X,Y,Z$ and $1 \times Z$) defined the reference datum. For points in the middle area of the object target field, the derived standard errors were found to be on

the order of $\sigma_X \simeq \sigma_Y \simeq 0.008$cm and $\sigma_Z \simeq 0.012$ cm. Expressing the internal accuracy as a ratio given by the standard error over the diameter of the object field, the precision in X and Y coordinate determinations is better than 1 part in 24,000. The precision of the Z coordinate determinations is somewhat less than this, being about 1 part in 16,000. The factor limiting the precision attainable with the Hasselblad MK-70 system and a multiple-camera self-calibration adjustment procedure is thought to be the large anomalous film deformation that remains regardless of the initial image coordinate transformation selected and regardless of the block-invariant additional parameter set adopted for the empirical image correction model. As mentioned, the RMS values of the photo coordinate residuals obtained in the multiple-camera self-calibration reported were of a magnitude of about 3.4 μm.

Conclusion

The method of simultaneous multiple-camera self-calibration outlined in the present paper has been employed in the calibration of a fixed-frame multiple-camera system designed for close-range photogrammetric survey applications in bioengineering and biomedicine. Among the salient attributes of the technique which became apparent in the fixed-frame system calibration are the increased degrees of freedom afforded in the multiple-camera self-calibration adjustment and the facility to accommodate camera-, block-, and image subset-invariant additional parameters in the image coordinate correction model.

Simultaneous multiple-camera self-calibration appears, from the results obtained in the reported investigation, to be a practical calibration technique for dual- and multiple-camera systems, and especially for photogrammetric systems designed for close-range applications.

References

Brown, D. C., 1972. Calibration of Close-Range Cameras. *Invited paper, XIIth Congress of ISP, Comm.* V, Ottawa.

Brown, D. C., 1974. Bundle Adjustment with Strip- and Block-Invariant Parameters, *Bildmessung und Luftbildwesen*, Vol. 42, pp. 210-220.

Brown, D. C., 1976. The Bundle Adjustment-Progress and Prospects, *Invited paper Comm. III, XIIIth Congress of ISP*, Helsinki.

Ebner, H., 1976. Self-Calibrating Block Adjustment, *Bildmessung und Luftbildwesen*, Vol. 44, No. 4, pp. 128-139.

El Hakim, S. F., and W. Faig, 1979. Combined Geodetic and Photogrammetric Adjustment for Densification of Control Networks, *Proc. ASP 45th Annual Meeting*, Washington, March, pp. 582-590.

Fraser, C. S., 1980. Multiple Focal Setting Self-Calibration of Close-Range Metric Cameras, *Photogrammetric Engineering and Remote Sensing*, Vol. 46, No. 9, pp. 1163-1173.

Gotthardt, E., 1975. Zusatzglieder bei der Aerotriangulation mit Bündeln, *Bildmessung und Luftbildwesen*, Vol. 43, No. 6, pp. 218-221.

Grün A., 1978. Experiences with Self-Calibrating Bundle Adjustment, *Presented paper ASP 44th Annual Meeting*, Washington, February.

Salmenperä, H., J. M. Anderson, and A. Savolainen, 1974. Efficiency of The Extended Mathematical Model in Bundle Adjustment, *Bildmessung und Luftbildwesen*, Vol. 42, No. 6, pp 229-233.

Schut, G., 1978. Selection of Additional Parameters for Bundle Adjustment, *Proc., ASP Fall Technical Meeting*, Albuquerque, pp. 490-503.

Veress, S. A., and R. S. Tiwari, 1976. Fixed-Frame Multiple Camera System for Close-Range Photogrammetry, *Photogrammetric Engineering and Remote Sensing*, Vol. 42, pp. 1195-1210.

(Received 18 July 1979; revised and accepted 27 May 1980)

Forthcoming Articles

Emily Bryant, Arthur G. Dodge, Jr., and *Samuel D. Warren*, Landsat for Practical Forest Type Mapping: A Test Case.

S. F. El Hakim and *W. Faig*, A Combined Adjustment of Geodetic and Photogrammetric Observations.

J. R. Gibson, A. J. Dow, and *S. E. Masry*, Adjustment of Position Using Inertial Navigation Systems.

Marilyn Hixson, Donna Scholz, Nancy Fuhs, and *Tsuyoshi Akiyama*, Evaluation of Several Schemes for Classification of Remotely Sensed Data.

Brent N. Holben, Compton J. Tucker, and *Jon W. Robinson*, A Ground-Based Spectral Technique for Determining Rain Forest Leaf Area Index.

E. Jeyapalan, Photogrammetry in Recording the Historic Ship Niantic.

D. S. Kimes, J. A. Smith, and *K. J. Ranson*, Vegetation Reflectance Measurements as a Function of Solar Zenith Angle.

Thomas J. Lauterborn, Aerial Photography Summary Record System—Five Years Later.

F. Ortí, Optimal Distribution of Control Points to Minimize Landsat Image Registration Errors.

P. R. Stephens, D. L. Hicks, and *N. A. Trustrum*, Aerial Photographic Techniques for Soil Conservation Research.

Dr. Craig H. Tom and *Dr. Lee D. Miller*, Forest Site Index Mapping and Modeling.